scientific reports

Check for updates

OPEN

Periplaneta americana extract improves recurrent oral ulcers through regulation of TLR4/NF-κB and Nrf2/HO-1 pathways

Weijun Li[1,3], Yi Chen[1,3], Kailing Li[2], Zhongze Chen[1], Jingyu Zhang[2], Guanhua Zhao[1], Fanfan Sun[1], Peiyun Xiao[1]✉ & Yongshou Yang[2]✉

Recurrent oral ulcers (ROUs) of oral mucosa disease are difficult to cure and relapse easily, and immune imLbalance or dysfunction is considered an essential factor in their occurrence and recurrence. *Periplaneta americana* extract (PAD), a raw material used in Kangfuxin Liquid and Yunnan Baiyao toothpaste, contains a variety of growth factors such as polypeptides and sticky sugar amino acids that promote tissue repair; this can encourage the growth of the granulation tissue and reduce inflammation on the wound surface. This study aimed to investigate the interventional potential of PAD on recurrent oral ulcers in rats and to elucidate the underlying mechanism of action involving the TLR4/NF-κB and Nrf2/HO-1 signaling pathways. A rat model of recurrent oral ulcer (ROU) was established using an oral antigen emulsifier. Rats in the ROU group were administered PAD by gavage for 7 days. To observe the effect of PDA on ROU mice. HE staining revealed that PAD restored the structure of the oral mucosal tissue and reduced inflammatory infiltration. FCM revealed that PAD upregulated CD3 + and CD4 + levels and the CD4 + /CD8 + ratio in peripheral blood T lymphocytes. ELISA revealed that PAD increased the content of IgA, IgG, IgM, VEGF, IL-2, and IL-10, while decreasing IL-6 and TNF-α content. Microplate analysis revealed that PAD significantly increased CAT content in the serum of ROU rats and reduced GSH, NO, SOD, and MDA levels. IHC staining, RT-qPCR, and Western blotting revealed that PAD downregulated Keap1 and IκBα expression, inhibited the TLR4/NF-κB signaling pathway, upregulated Nrf2 and HO-1 expression, and activated the Nrf2/HO-1 signaling pathway. These fndings suggest that PAD improved immune imbalance and oxidative stress in ROU rats by activating the Nrf2/HO-1 pathway and inhibiting the TLR4/NF-κB signaling pathway, thereby promoting the healing of oral ulcer wounds.

Keywords *Periplaneta americana* extract, Recurrent oral ulcer, Immune regulation, TLR4/NF-κB signaling pathway, Nrf2/HO-1 signaling pathway

Recurrent oral ulcer (ROU) is a chronic inflammatory mucosal lesion that presents with one or more erosions or ulcers on the lips, tongue, and buccal mucosa[1]. It is prevalent in up to 25% of the general population and is accompanied by severe pain and inflammation that affects patients' daily lives[2].

The occurrence of ROU is related to internal and external environmental conditions. The internal causes include abnormal immunological, digestive, and metabolic function, while the external causes include viral infection and psychological stress[3–5]. Given its numerous etiologies, most scholars regard ROU as a disease related to immune-function status, and immune imbalance or dysfunction is considered an essential factor for its occurrence and recurrence[6,7]. Consequently, investigating the immunological function of patients is the most recent research focus in understanding the pathogenesis of ROU. Anomalies in T-lymphocyte subsets (including $CD3^+$, $CD4^+$, and the $CD4^+/CD8^+$ ratio) in the peripheral blood of ROU patients cause aberrant release of cytokines (like IL-2, -6, and -10), as well as tumor necrosis factor-alpha (TNF-α), which in turn sets off an immunological reaction in the body[1,8]. In inflammatory reactions, nuclear factor-kappa B (NF-κB) and its signaling pathway participate in the immune process as an essential nuclear transcription factor. IL-6 and TNF-α

[1]Engineering Research Center for Development of the Periplaneta Americana Industry of Yunnan Provincial Department of Education, Dali University, Dali 671000, Yunnan, China. [2]College of Pharmacy, Dali University, Dali 671000, Yunnan, China. [3]Weijun Li and Yi Chen have contributed equally. ✉email: xiaopeiyun@dali.edu.cn; yangyongshou@dali.edu.cn

gene promoters present at the corresponding binding sites of NF-κB activate the NF-κB signaling pathway through NF-κB-inducing kinase[9]. Experiments conducted in vitro and in vivo have verified that sustained activation of NF-κB leads to an increase in the secretion of TNF-α, IL-6, IL-1β, and other associated factors, which in turn stimulate the immunological response of the body[10,11]. In addition, the pathogenesis mentioned above can directly or indirectly disrupt oxidative and antioxidant balance in the body. Disruption of this balance accelerates the generation and accumulation of free radicals, leading to severe cellular damage[12–14].

Excessive levels of reactive oxygen species (ROS) attack the oral mucosa, impairing normal cell function and structural integrity and leading to frequent ulcers[15]. Nuclear factor erythroid 2-related factor 2 (Nrf2), in the cap-n-collar family of transcription factors, is a key transcription factor in the cellular regulation of oxidative stress, owing to its high sensitivity to oxidative stress[16]. Normally, Nrf2 conjugates with the Kelch-like ECH-associated protein1 (Keap1) to reduce Nrf2 activity. Externally stimulated Nrf2 is uncoupled from Keap1 and transferred into the nucleus, where it initiates the expression of genes involved in phase II detoxification and antioxidant enzymes under the regulation of antioxidant response elements, enhancing cellular resistance to oxidative stress[17].*Periplaneta americana* (Arthropoda, Insecta, Blattaria, Blattidae) is currently the only cockroach developed for medicinal purposes. Extensive pharmacological investigations have revealed that *P. americana* promotes tissue repair, exhibits antioxidant properties, mitigates inflammation, and boosts immune function[18–20]. Kangfuxin liquid (approval number: National Medicine Zhunzi Z51021834), a unilateral preparation from *P. americana* extract that is commonly used clinically to treat a variety of diseases, including trauma, bedsores, and gastrointestinal ulcers, exhibits remarkable curative effects[21]. Reportedly, Kangfuxin liquid can regulate the ratios of $CD3^+$, $CD4^+$, and $CD8^+$ in patients' peripheral blood, as well as the expression of TNF-α, IL-6, and IL-8, which has a significant therapeutic effect on patients with radioactive oral ulcer[22] (Wang, 2021). The results above suggest that Kangfuxin liquid can effectively heal oral ulcers in patients with cancer. The underlying therapeutic mechanism may regulate the immune function and ameliorate inflammatory responses. Our research group established an early-stage ulcer model of phenol-injured rat oral mucosa and found that PAD, the raw material of Yunnan Baiyao "active peptide toothpaste," industry-standard number: QB/T5287-218) has a good therapeutic effect on acute oral ulcers in rats[23]. However, the therapeutic effect and mechanism of action of the PAD on ROU remains unclear.

Based on these findings, we constructed an ROU rat model using an oral antigen emulsifier to investigate the mechanisms by which *P. americana* extract (PAD) promotes the healing of oral ulcers by regulating immune function and reducing inflammation and oxidation. Specifically, we investigated the pivotal role of the Nrf2/Hemoxygenase-1 (HO-1) and Toll-like receptor 4 (TLR4)/NF-κB signaling pathways and provided experimental data supporting the further development and application of *P. americana* extract.

Results

Primary components of PAD

PAD composition was determined via UPLC-Q-TOF–MS. Figure 1A and 1B show the total ion chromatograms for positive and negative ions, respectively. Based on database comparison, forty compounds were identified in PAD (Table 1). These compounds included 7 amino acids, 7 alkaloids, 6 fatty acids, 5 nucleosides, 4 peptides, 3 sugars, and 8 other compounds. The structures of the identified compounds are presented in Fig. 2.

PAD improved oral ulcer tatus and pathological structure of oral mucosa in ROU rats

After four weeks of modeling, the oral mucosa of the rats in the control group was intact, with a bright red and glossy color, and there was no ulcer formation. However, the model rats exhibited swollen oral horns, moist lips, salivation, and white ulcer spots in the oral mucosa. After 6 weeks of modeling, oral administration was performed for 7 days. Compared with the control group, the number, duration, and area of ulcers increased significantly in the model group ($P<0.01$) (Fig. 3A–C). Compared with the model group, the number, duration, and area of ulcers in all drug groups were significantly reduced ($P<0.05$). Both PAD and LM relieved the symptoms, and the PAD-H group had only local redness and swelling around the oral mucosal tissue, without obvious ulcers, suggesting that PAD has a specific therapeutic effect on ROU in rats. HE staining of the rat oral mucosae is shown in Fig. 3D. In the control group, the oral mucosa was integrated, and the epithelial cells of the mucosal layer were arranged neatly, with clear layers and structures in the mucosal epithelial layer, basement membrane, and lamina propria. Oral mucosal ulcers were apparent in the model group, with some necrotic and exfoliating epithelial cells, resulting in epithelial damage and disordered cell arrangement accompanied by inflammatory cell infiltration. The mucosal epithelial cell layer was exfoliated and defective in the PAD-L and

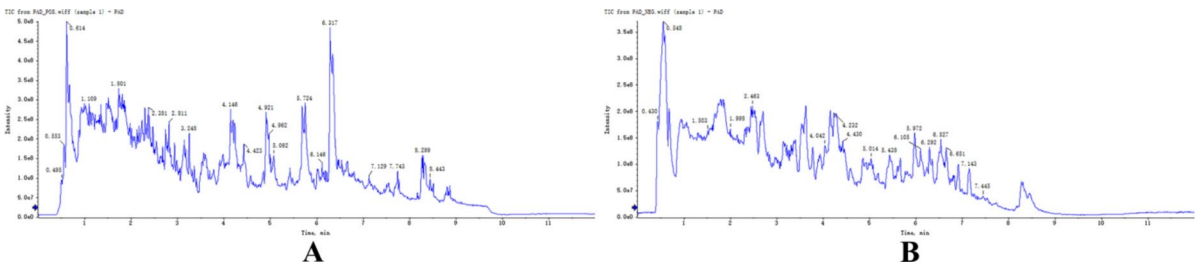

Fig. 1. Total ion chromatogram of PAD in positive (**A**) and negative (**B**) ion modes.

No	RT (min)	Compounds	Formula	Molecular weight (Da)	Precursor m/z	Ionization model
1	0.430	Hydroquinone	$C_6H_6O_2$	110.11	109.03	$[M-H]^-$
2	0.495	2-Phenylacetamide	C_8H_9NO	135.16	136.08	$[M+H]^+$
3	0.548	Dl-benzylsuccinic acid	$C_{11}H_{12}O_4$	208.21	207.00	$[M-H]^-$
4	0.553	1-palmitoyl-2-oleoyl-sn-glycerol	$C_{37}H_{70}O_5$	594.90	595.53	$[M+H]^+$
5	0.614	Erucamide	$C_{22}H_{43}NO$	337.60	338.34	$[M+H]^+$
6	0.678	Oleic acid	$C_{18}H_{34}O_2$	282.50	281.25	$[M-H]^-$
7	1.109	Niacinamide	$C_6H_6N_2O$	122.12	123.06	$[M+H]^+$
8	1.503	Uracil	$C_4H_4N_2O_2$	112.09	111.00	[M-H]-
9	1.801	S-methyl-5′-thioadenosine	$C_{11}H_{15}N_5O_3S$	297.34	298.00	$[M+H]^+$
10	1.998	2-methylbenzoic acid	$C_8H_8O_2$	136.15	135.00	$[M-H]^-$
11	2.381	1,2-dilinoleoyl-sn-glycero-3-phosphocholine	$C_{44}H_{80}NO_8P$	782.10	783.00	$[M+H]^+$
12	2.463	Sinapoylhexoside	$C_{17}H_{22}O_{10}$	386.30	385.11	$[M-H]^-$
13	2.811	Oleoyl-l-carnitine	$C_{25}H_{47}NO_4$	425.60	426.36	$[M+H]^+$
14	3.145	1-oleoyl-sn-glycero-3-phosphocholine	$C_{26}H_{52}NO_7P$	521.70	522.36	$[M+H]^+$
15	3.248	3′-o-methylguanosine	$C_{11}H_{15}N_5O_5$	297.27	298.11	$[M+H]^+$
16	3.771	Thr-Leu	$C_{10}H_{20}N_2O_4$	232.28	231.14	[M-H]-
17	4.042	1,11-undecanedicarboxylic acid	$C_{13}H_{24}O_4$	244.33	243.16	$[M-H]^-$
18	4.146	Pyrimethamine	$C_{12}H_{13}ClN_4$	248.71	249.09	$[M+H]^+$
19	4.232	Ala-Ile	$C_9H_{18}N_2O_3$	202.25	201.12	$[M-H]^-$
20	4.423	Trimethylamine	C_3H_9N	59.11	60.08	$[M+H]^+$
21	4.430	Acetyl-DL-Valine	$C_7H_{13}NO_3$	159.18	158.08	$[M-H]^-$
22	4.921	DL-tyrosine	$C_9H_{11}NO_3$	181.19	182.08	$[M+H]^+$
23	4.962	Acetylcarnitine	$C_9H_{17}NO_4$	203.24	204.12	$[M+H]^+$
24	5.014	N-fructosyl isoleucine	$C_{12}H_{23}NO_7$	293.31	292.14	$[M-H]^-$
25	5.062	DL-proline	$C_5H_9NO_2$	115.13	116.07	$[M+H]^+$
26	5.438	Uric acid	$C_5H_4N_4O_3$	168.11	167.02	$[M-H]^-$
27	5.725	L-carnitine	$C_7H_{15}NO_3$	161.20	162.11	$[M+H]^+$
28	5.972	2,3-dihydroxybenzoic acid	$C_7H_6O_4$	154.12	153.02	$[M-H]^-$
29	6.105	Glutamine	$C_5H_{10}N_2O_3$	146.14	145.06	$[M-H]^-$
30	6.146	DL-histidine	$C_6H_9N_3O_2$	155.15	156.08	$[M+H]^+$
31	6.292	Glycerol 3-phosphate	$C_3H_9O_6P$	172.07	171.01	$[M-H]^-$
32	6.317	Glycerophosphocholine	$C_8H_{20}NO_6P$	257.22	258.11	$[M+H]^+$
33	6.527	O-phosphoethanolamine	$C_2H_8NO_4P$	141.06	140.00	$[M-H]^-$
34	6.651	Maltitol	$C_{12}H_{24}O_{11}$	344.31	343.12	$[M-H]^-$
35	7.129	Pyroglu-ser-lys	$C_{14}H_{24}N_4O_6$	344.36	345.18	$[M+H]^+$
36	7.143	Uridine 5′-monophosphate	$C_9H_{13}N_2O_9P$	324.18	323.03	$[M-H]^-$
37	7.445	Raffinose	$C_{18}H_{32}O_{16}$	504.40	503.51	$[M-H]^-$
38	7.743	Phosphocholine	$C_5H_{15}NO_4P$	184.15	185.00	$[M+H]^+$
39	8.299	L-ng-monomethylarginine	$C_7H_{16}N_4O_2$	188.23	189.13	$[M+H]^+$
40	8.443	Arginine	$C_6H_{14}N_4O_2$	174.20	175.12	$[M+H]^+$

Table 1. Preliminary identification of compounds in PAD (positive/negative).

LM groups. In the PAD-H group, the structure of the mucosal epithelial layer was intact, with some submucosal duct lumens slightly dilating. The therapeutic effect of PAD-M was intermediate between that of PAD-L and PAD-H. These results indicate that the PAD effectively improved the pathology of the oral mucosa of ROU rats.

PAD improves immune function in ROU rats

The effects of PAD on the immune indices of ROU rats are shown in Fig. 4. Compared with the control group, the proportions of $CD3^+$ and $CD4^+$ cells and the $CD4^+/CD8^+$ ratio were significantly lower in the model group ($P<0.05$) (Fig. 4A, B), whereas those of $CD8^+$ cells did not differ among groups. Serum IgA, IgG, and IgM levels were significantly elevated in the model group ($P<0.01$) (Fig. 4C–E). Compared with the model, drug intervention significantly upregulated $CD3^+$ and $CD4^+$ cell levels, the $CD4^+/CD8^+$ ratio, and downregulated IgA, IgG, and IgM levels ($P<0.05$). The results indicate that PAD regulated the ratios of T lymphocyte-subset levels to immunoglobulin content, thus regulating the balance of immune function in ROU rats.

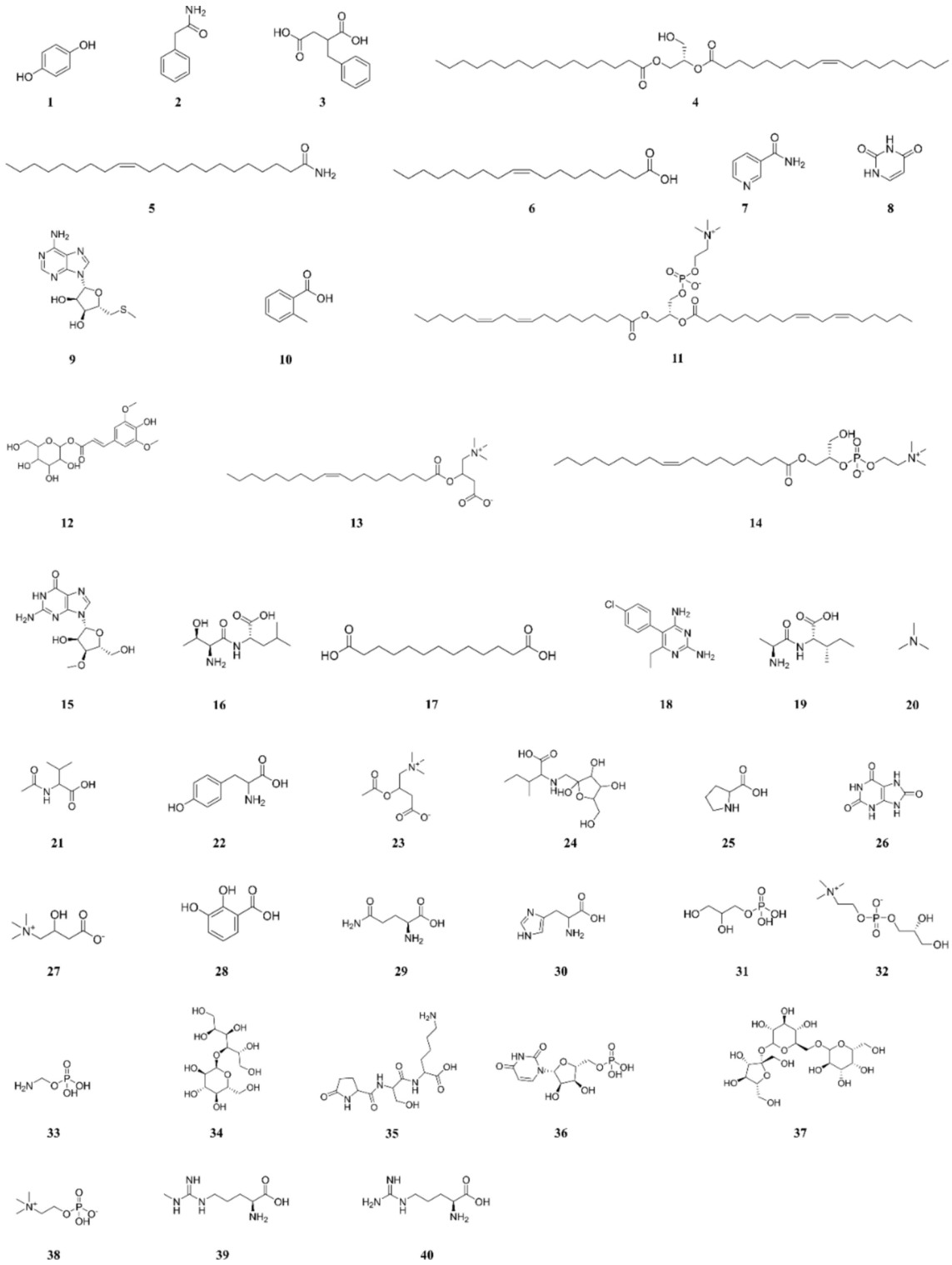

Fig. 2. Chemical structures of the 40 compounds in PAD.

PAD Inhibits inflammation and promotion of ulcer healing in ROU rats

Based on ELISA, IL-6, TNF-α, VEGF, IL-10, and IL-2 levels are shown in Fig. 5A–E. Compared with the control group, serum IL-6, TNF-α, and VEGF were significantly elevated in the model group, while serum IL-2 and IL-10 were significantly reduced ($P < 0.05$). Compared with the model, after treatment with PAD and LM, serum IL-6 and TNF-α were significantly reduced, while those of VEGF, IL-2, and IL-10 were significantly elevated ($P < 0.05$). The RT-QCPR results are shown in Fig. 5F–H. Compared with the control, TNF-α, VEGF, and IL-1β mRNA levels were elevated in the oral mucosa of the model group ($P < 0.05$). Compared with the model group,

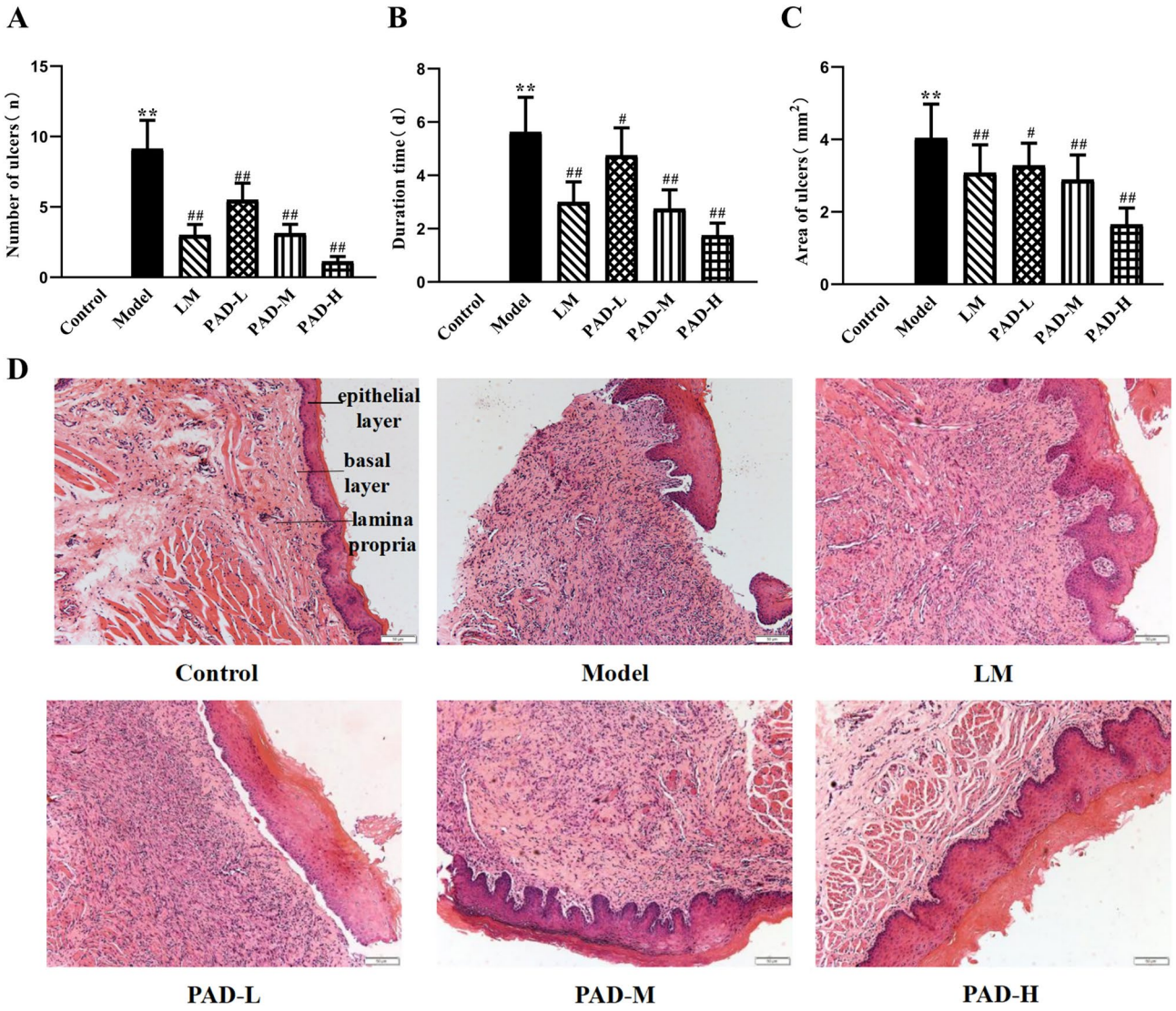

Fig. 3. PAD improved oral ulcer tatus and pathological structure of oral mucosa in ROU rats. (**A–C**) Comparison of oral ulcer status of ROU rats in each group (n = 8). (**D**) HE staining plots (200 × magnification). (Date are Mean ± SD: $^{*}P < 0.05$, $^{**}P < 0.01$ versus. the control group; $^{\#}P < 0.05$, $^{\#\#}P < 0.01$ versus the model group).

the PAD and LM groups exhibited upregulated mRNA expression of VEGF, while TNF-α and IL-1β mRNA expression was downregulated, further validating the ELISA results and demonstrating that PAD effectively inhibited the local inflammatory response in the oral cavity of ROU rats, promoted oral mucosal epithelial cell proliferation, and accelerated ulcer healing.

PAD improves oxidative stress injury in the oral cavity of ROU rats

Compared with the control, serum CAT was significantly lower in the model ($P < 0.01$), while serum GSH, SOD, NO, and MDA levels were significantly higher ($P < 0.01$) (Fig. 6A–E). Treatment with PAD and LM increased CAT content; the CAT content in the PAD-H group approached that in the control group ($P < 0.05$). Moreover, PAD and LM reduced the elevated GSH, SOD, NO, and MDA content caused by the antigen emulsifier. This implies that PAD inhibits oxidative damage to the oral mucosa in ROU rats.

PAD inhibited the TLR4/NF-κB signaling pathway in the oral mucosa of ROU rats

RT-qPCR detection revealed that TLR4, IKKβ, NF-κB p50, NF-κB p65, and IκBα mRNA expression was higher in the oral mucosa tissue in the model than in the control group ($P < 0.01$). Furthermore, it was lower in the PAD and LM groups, and particularly in the PAD-H group, than in the model ($P < 0.01$) (Fig. 7A–E). Western blotting of TLR4, MyD88, TRAF6, NF-κB p50, NF-κB p65, and IκBα in the oral mucosa tissue validated the patterns observed in their mRNA expression (Fig. 7F–L). The results of IHC to detect NF-κB p50 and IκBα protein expression in the oral mucosal tissue were consistent with the Western blotting results (Fig. 7M–O). PAD effectively downregulated TLR4, MyD88, TRAF6, NF-κB p50, NF-κB p65, and IκBα gene expression, and

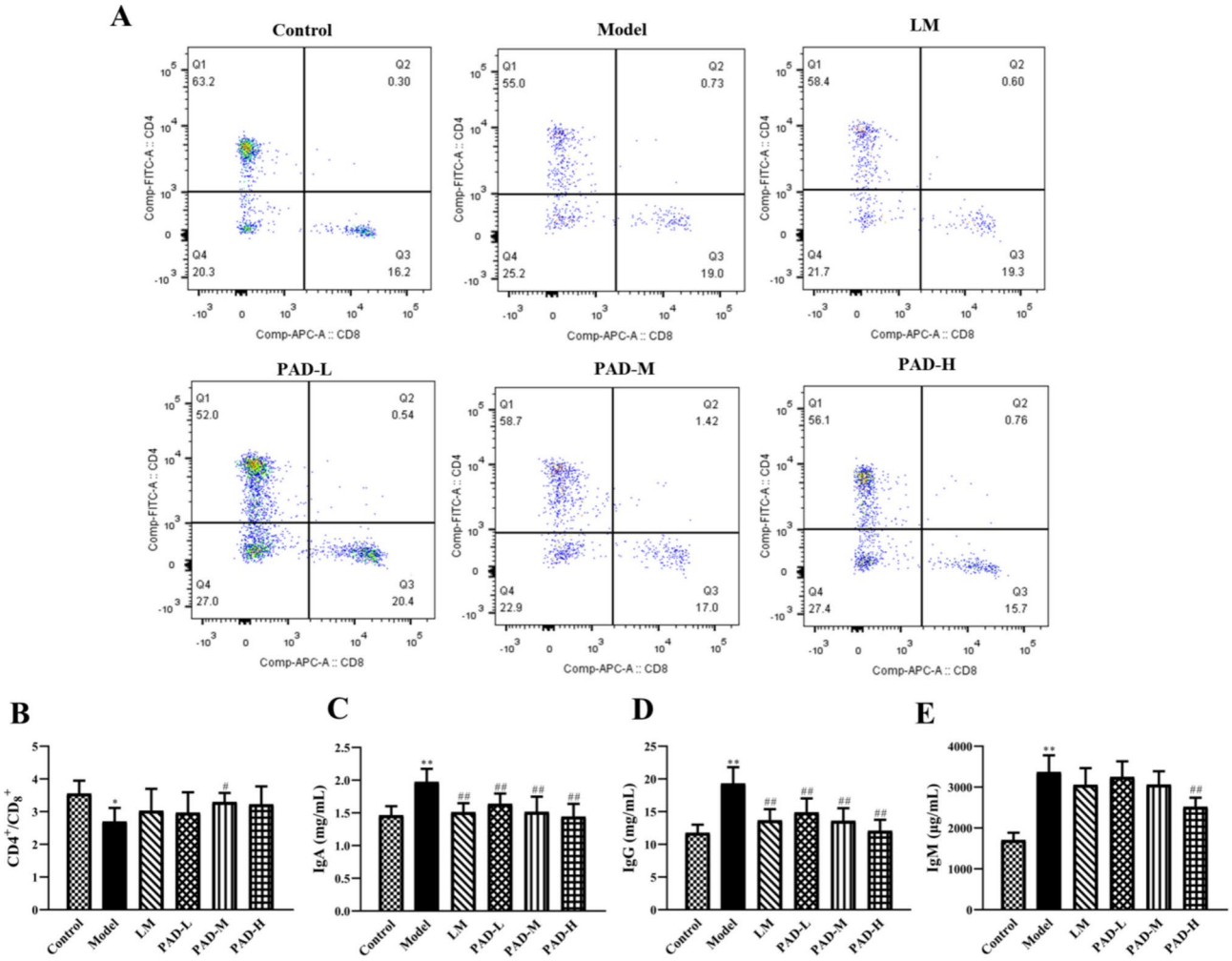

Fig. 4. PAD regulation of immune function in ROU rats. (**A**) Flow scatter diagram: Positive expression of $CD4^+$ and $CD8^+$ cells in peripheral blood. (**B**) Measurement of the $CD4^+/CD8^+$ ratio in the peripheral blood of rats in each group using flow cytometry (n = 5). (**C–E**) Determination of serum IgA, IgG, and IgM in each group, using ELISA (n = 8). (Date are Mean ± SD: $^{*}P < 0.05$, $^{**}P < 0.01$ versus. the control group; $^{\#}P < 0.05$, $^{\#\#}P < 0.01$ versus the model group).

the protein expression of the proteins involved in the TLR4–NF-κB signaling pathway in the oral mucosa of the ROU rats. This implies that PAD achieves its therapeutic effects in ROU by inhibiting TLR4/NF-κB signaling.

PAD activates the Nrf2/HO-1 signaling pathway in the oral mucosa of ROU rats

Gene expression based on RT-qPCR is shown in Fig. 8A–E. The mRNA expression of Nrf2, Keap1, NQO1, HO-1, and CAT in the oral mucosal tissue was significantly lower in the model than in the control ($P < 0.01$), and PAD and LM treatment increased their expression to varying degrees. Western blotting revealed that Nrf2, Keap1, NQO1, and HO-1 expression in the oral mucosa was significantly lower in the model than in the control ($P < 0.01$) and was higher after treatment with PAD and LM (Fig. 8F–J). IHC of oral mucosal tissue revealed that Keap1, NQO1, and HO-1 were concentrated in the cytoplasm, exhibiting yellow or brownish-yellow positive expression (Fig. 8H). Compared with the control, Keap1, NQO1, and HO-1 expression was significantly lower in the model ($P < 0.01$). After treatment, the extent of Keap1, NQO1, and HO-1 positivity increased, especially in the PAD-M and PAD-H groups ($P < 0.05$; Fig. 8I–N). These results suggest that PAD upregulated the gene and protein expression of Nrf2, Keap1, NQO1, and HO-1, which are underexpressed in the Nrf2/HO-1 signaling pathway in the oral mucosa of ROU rats, reflecting the good antioxidant effects of PAD. Therefore, we speculate that the mechanism of PAD-induced ulcer repair in ROU rats is related to the activation of the Nrf2/HO-1 signaling pathway.

Discussion

ROU, a common oral mucosal disease that causes local pain, has a high incidence and recurrence rates[24]. At the onset of ROU, the epithelial cells are stimulated by lymphocyte infiltration and inflammation, triggering local tissue edema. In ROU, activation of T cells and TNF-α is mediated by leukocytes, macrophages, and mast cells to

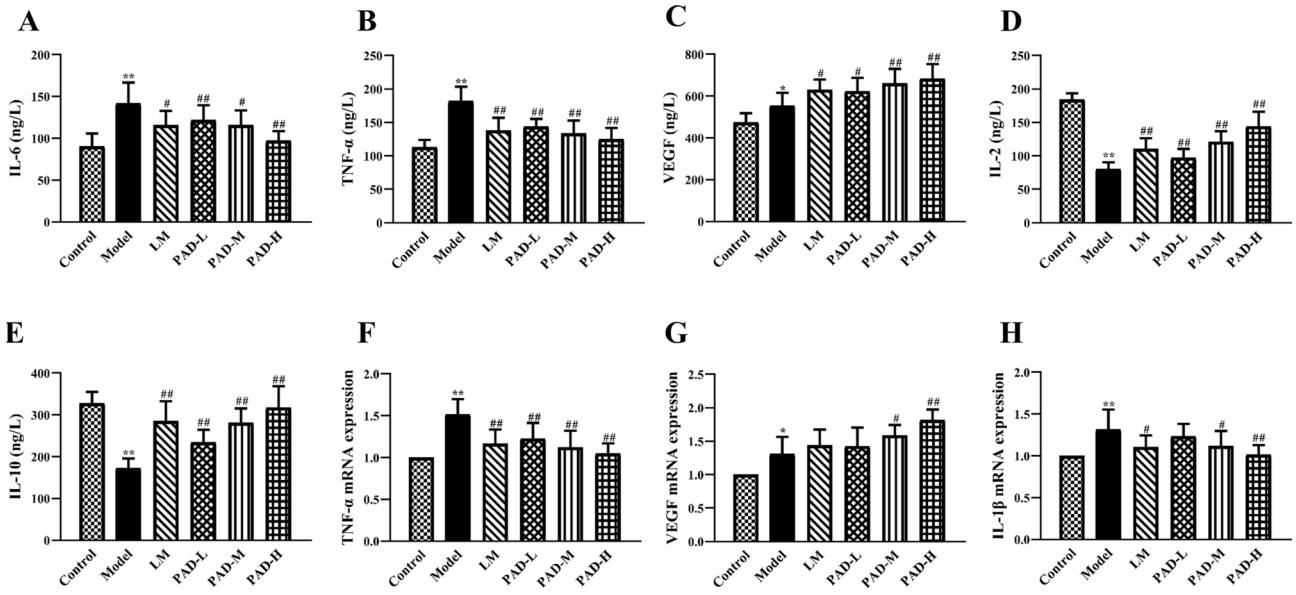

Fig. 5. Inhibition of oral inflammation and promotion of ulcer healing by PAD in ROU rats. (**A–E**) Serum IL-6, TNF-α, VEGF, IL-2, and IL-10, via ELISA (n = 8). (**F–H**) RT-qPCR detection of TNF-α, VEGF, and IL-1β mRNA levels in the oral mucosa (n = 5). (Date are Mean ± SD: $^{*}P < 0.05$, $^{**}P < 0.01$ versus. the control group; $^{\#}P < 0.05$, $^{\#\#}P < 0.01$ versus the model group).

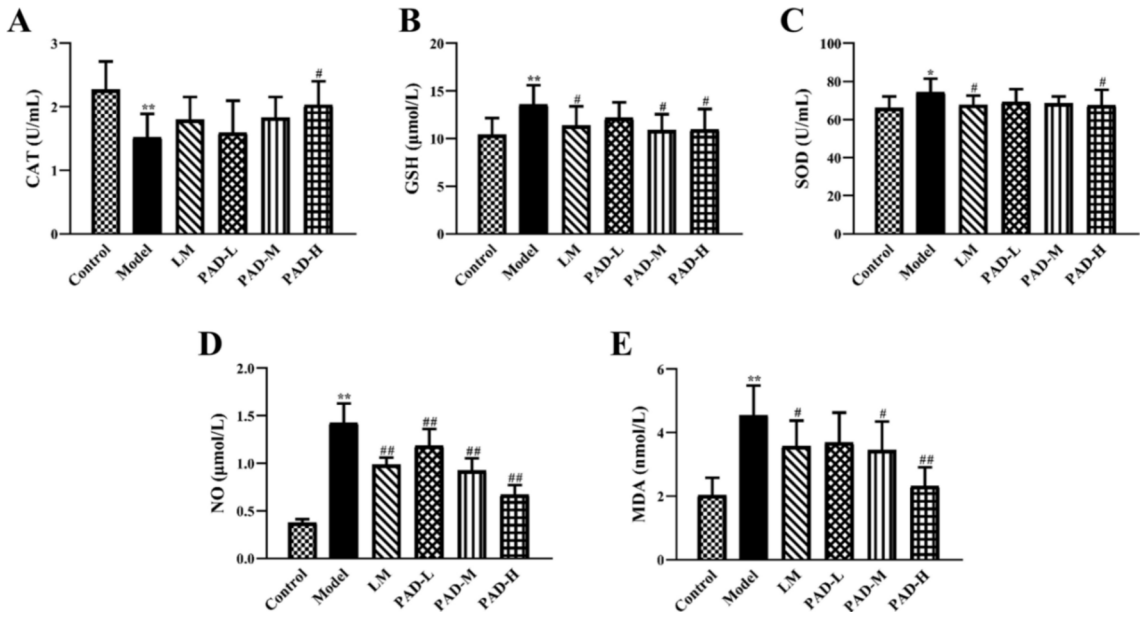

Fig. 6. Amelioration of oral oxidative stress injury in ROU rats treated with PAD. (**A–E**) Serum levels of the oxidative stress markers CAT, GSH, SOD, NO, and MDA via microplate assay (n = 8). (Date are Mean ± SD: $^{*}P < 0.05$, $^{**}P < 0.01$ versus. the control group; $^{\#}P < 0.05$, $^{\#\#}P < 0.01$ versus the model group).

activate the immune response[25]. This process may involve a cell-mediated immune response. Patients with ROU exhibit varying degrees of cellular immune dysfunction, in which the levels of cytokines such as IL-2, IL-6, and TNF-α produced by T-lymphocyte subsets are imbalanced and functionally altered[26,27].

LM is commonly used to treat ROU. Therefore, to enable parallel comparison with the outcomes observed in clinical cases, we chose LM as the positive agent. LM is an immunomodulator that contains two pharmacologically active molecular structures: an imidazole ring and a sulfur-containing region. LM plays a bidirectional regulatory role in humoral immune abnormalities by regulating and restoring immunity, thereby restoring immune function[28].

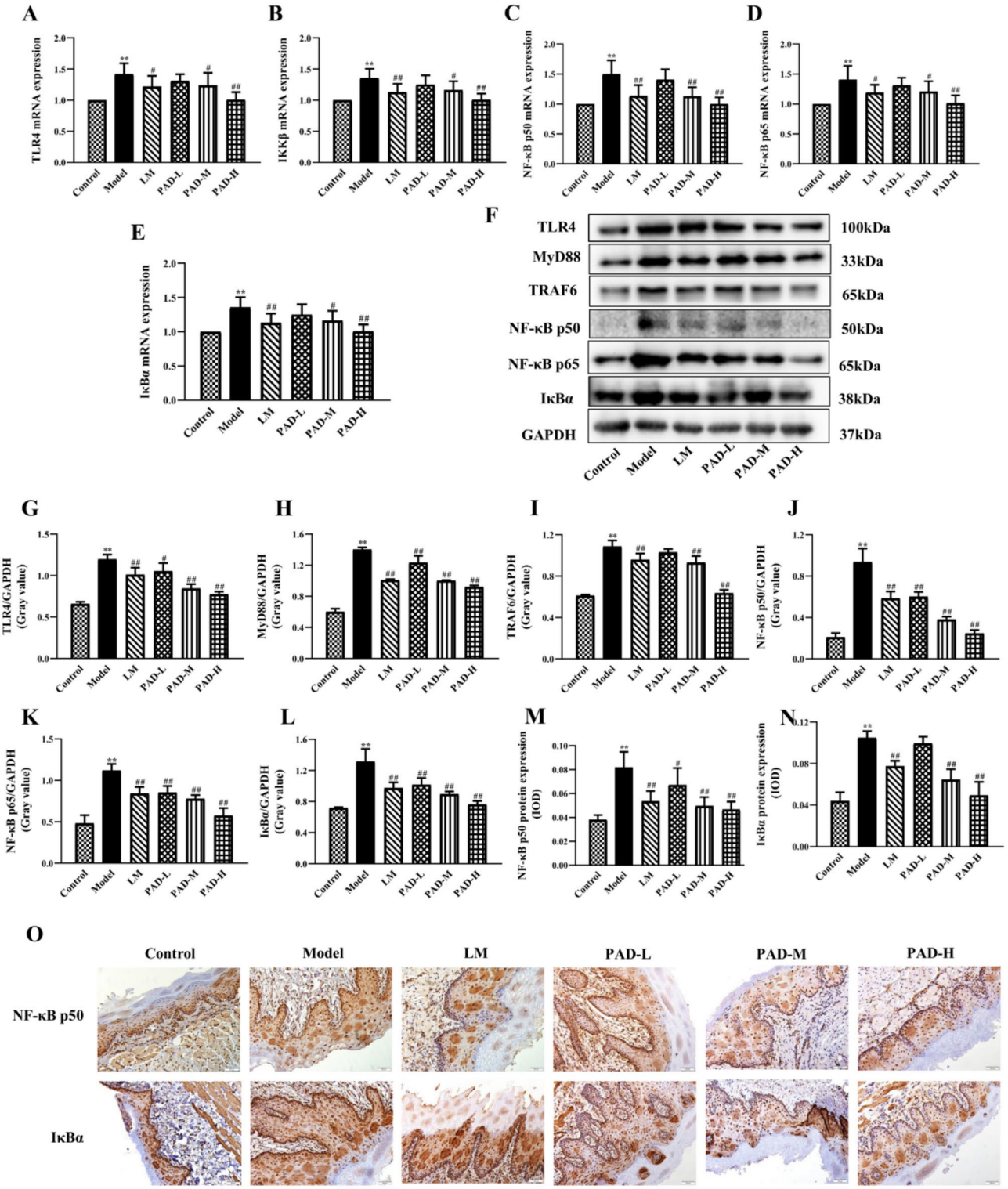

Fig. 7. Inhibition by PAD of TLR4/NF-κB signaling in the oral mucosa of ROU rats. (**A–E**) RT-qPCR detection of mRNA expression of TLR4/NF-κB pathway-related genes in the oral mucosa (n = 5). (**F**) Western blot electrophoretogram of TLR4/NF-κB pathway-related proteins. (**G–L**) Determination of TLR4/NF-κB pathway-related protein expression in the oral mucosa via Western blotting. (**M–N**) NF-κB p50 and IκBα expression levels in the oral mucosa via IHC. (**O**) Immunohistochemical staining plots (NF-κB p50 and IκBα; 200 × magnification). (Date are Mean ± SD: $^{*}P < 0.05$, $^{**}P < 0.01$ versus. the control group; $^{\#}P < 0.05$, $^{\#\#}P < 0.01$ versus the model group).

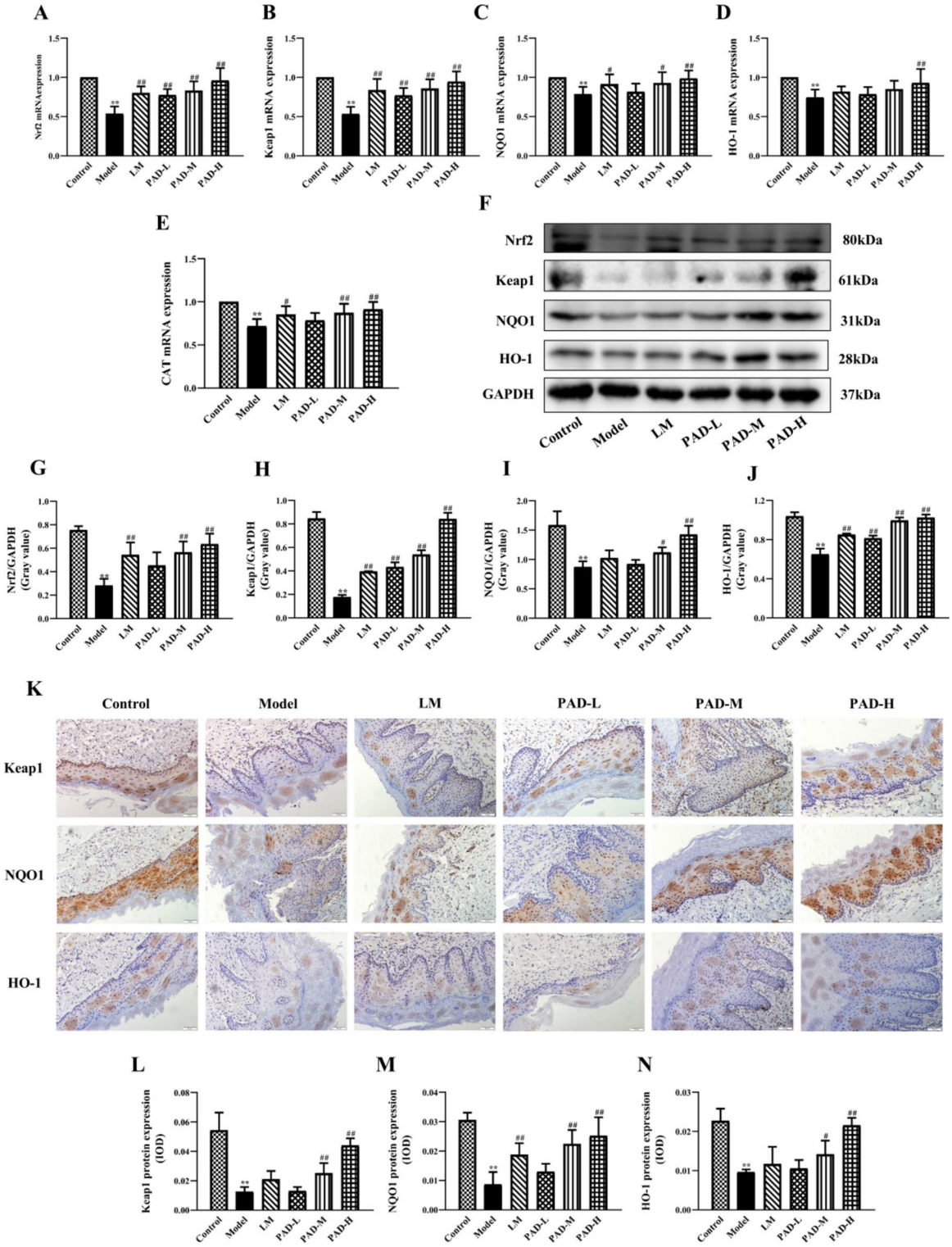

Fig. 8. PAD facilitates ulcer healing in ROU rats by activating the Nrf2/HO-1 signaling pathway. (**A–E**) RT-qPCR-based detection of Nrf2, Keap1, NQO1, HO-1, and CAT mRNA expression in the Nrf2/HO-1 signaling pathway in the oral mucosa of rats in each group (n = 5). (**F**) Western blotting electrophoretogram of Nrf2/HO-1 pathway-related proteins. (**G–J**) Western blotting analysis of Nrf2, Keap1, NQO1, and HO-1 expression in the Nrf2/HO-1 signaling pathway in the oral mucosa. (**H**) Immunohistochemical staining of Keap1, NQO1, and HO-1 (200 × magnification). (**I–K**) Immunohistochemical staining analysis of Keap1, NQO1, and HO-1 expression in the oral mucosa. (**L–N**) Keap1, NQO1 and HO-1 expression levels in the oral mucosa via IHC. (Date are Mean ± SD: $^{*}P < 0.05$, $^{**}P < 0.01$ versus. the control group; $^{\#}P < 0.05$, $^{\#\#}P < 0.01$ versus the model group).

In this study, we generated an ROU rat model using an oral antigen emulsifier. This model is suitable for studying the occurrence and mechanisms of the development of ROU because it is similar to the pathogenesis of human ROU[29]. Over time, the ROU model rats gradually displayed dull fur and became easier to provoke; their weight gain slowed, and they exhibited moist and drooling lips, as well as prominent redness and swelling of the oral mucosa with tiny white ulcers. Under light microscopy (HE staining), the epithelial cell layer of the oral mucosa was clearly detached and defective, with inflammatory cell infiltration, indicating that the model was successful. After treatment with PAD and LM, all symptoms were alleviated, especially in the PAD-H group, which showed the most significant effects and tended to be normal, suggesting that PAD improves the pathological structure of the oral mucosa in ROU rats and promotes repair of oral ulcer wounds.

T and B lymphocytes are the main cellular components of the peripheral immune system and work together to effectively identify and eliminate harmful substances in the body. Under normal circumstances, the $CD4^+$ and $CD8^+$ T-lymphocyte subsets are in a state of balance. The $CD4^+/CD8^+$ ratio, therefore, remains stable within a specific range, and the synergistic effect of subsets is important for maintaining the immune function of the body. In patients with ROU, disruption of this homeostasis reduces the immune function of the body or local cells and promotes apoptosis of the oral mucosal epithelium, which triggers damage and necrosis of the epithelial tissues, ultimately leading to localized oral mucosal ulceration[30,31]. A previous study showed that the proportion of T-lymphocyte subsets is significantly altered in the lesion area and peripheral blood of patients with ROU and that $CD4^+$ lymphocytes were predominant in the early and recovery stages of the disease, while $CD8^+$ lymphocytes were dominant in the pathogenic phase of the disease[32]. It can be seen that the occurrence of ROU is associated with an imbalance in the number of lymphocyte subsets and with a change in function. The results of the present study revealed a significant downregulation of CD3 and CD4, and of the $CD4^+/CD8^+$ ratio, in the blood of ROU rats in the model group compared with the control group ($P<0.05$), in accordance with the previous clinical findings of Chen et al[33]. However, in the rats of the PAD group, $CD3^+$ and $CD4^+$ cell levels and the $CD4^+/CD8^+$ ratio were significantly elevated, indicating that the PAD effectively regulated the expression of T lymphocytes, thus regulating the balance of immune function in ROU rats.

The immunoglobulins secreted by B cells are primarily IgA, IgG, and IgM. Secretion of IgA, IgG, and IgM is regulated by the entire immune system. Abnormal immune function causes abnormal levels of IgA, IgG, and IgM in the body, ultimately disrupting the balance between various cytokines. Therefore, changes in immunoglobulin levels can be used as important indicators to evaluate disease conditions. In the present study, the levels of IgA, IgG, and IgM were significantly higher in the model group, consistent with the findings of a clinical study by Li et al[34]. PAD increased and corrected the levels of immunoglobulins in the serum of ROU rats, indicating that PAD could regulate the expression of immunoglobulins in the serum to maintain the balance of immune function in ROU rats, thus playing a therapeutic role.

IL-2 is a signaling molecule that regulates lymphocyte activity in the immune system and is mainly secreted by activated $CD4^+$ lymphocytes, which can promote T cells from the G1 phase to the S phase and accelerate the replication and proliferation of T cells[35]. Our results showed that serum IL-2 was significantly lower in the model than in the control ($P<0.05$), and peripheral blood $CD4^+$ T-lymphocyte levels were also lower. The levels of IL-2 were regulated by $CD4^+$ T lymphocytes, and these two results were corroborated. PAD rescued serum IL-2 in the model, indicating that PAD has a regulatory effect on $CD4^+$ cells.

IL-10 can activate B cells, inhibit Th1 cell and macrophage activity, and stimulate antibody secretion, thereby regulating the immune response[36]. IL-10 protein and mRNA levels are low in the oral mucosa of patients with ROU; this reduction in IL-10 suppresses the normal cellular immune response and affects the progression of ROU[24]. In this study, serum IL-10 was significantly decreased in the model ($P<0.05$); this reduction is not conducive to the proliferation and tissue remodeling of mucosal epithelial cells. PAD increased serum IL-10 in the model, enhancing innate immunity, inhibiting the inflammatory response, and accelerating ulcer healing.

In the immune response to inflammation, IL-6, IL-1β, and TNF-α are the primary immune activators[37]. IL-6 causes the formation of chemotactic adhesion molecules, recruits monocytes to diseased tissues, induces the manufacture and secretion of numerous cytokines, and affects cell growth and apoptosis[38]. IL-1β can increase the recruitment of granulocytes, activate natural immune lymphocytes, promote the occurrence of natural immune diseases, and accelerate the activity of transcription pro-inflammatory cytokines. TNF-α accumulation acts on epithelial cells to enhance adhesion, inducing the chemotactic migration of neutrophils to the lesion site and activating cytotoxic T cells and neutrophils, leading to epithelial cell necrosis[39]. TNF-α content is significantly higher in the saliva of patients with ROU than in that of patients without ROU, suggesting that TNF-α can be used as a biomarker to evaluate both ROU progression and deterioration and the therapeutic impact of drugs[40]. Mei et al[41]. found that serum pro-inflammatory factor (TNF-α, IL-1β, and IL-6) levels were significantly higher in ROU rats than in normal rats, while IL-10 content was significantly lower and that the ROU rats exhibited significantly higher NF-κB p65 protein expression in the oral mucosal tissue. This demonstrates that activation of NF-κB signaling promotes the synthesis and secretion of pro-inflammatory factors during ROU while inhibiting IL-10 synthesis and secretion. Our findings are similar to those reported in the literature. Serum IL-6 and TNF-α and the oral mucosal mRNA expression of TNF-α and IL-1β were significantly elevated in the model ($P<0.01$), while IL-10 expression was significantly reduced, indicating an inflammatory reaction in the oral cavity of ROU rats. HE results revealed severe inflammatory infiltration in the oral mucosal tissue of the model, consistent with the observed elevated inflammatory mediator levels. In the model, PAD inhibited the inflammatory response in the oral cavity and effectively reduced both IL-6 and TNF-α levels and TNF-α and IL-1β mRNA expression.

VEGF, a specific provascular endothelial cell mitogen, regulates the migration and proliferation of capillary endothelial cells and plays a vital role in maintaining the normal state and integrity of blood vessels[42]. In addition, VEGF is a significant mediator of neoangiogenesis in the granulation tissue of ulcer wounds, and its protein expression is closely related to neovascularization and wound healing[43]. Our study found that in the model, with an increase in PAD oral dosage, serum VEGF and mRNA expression levels in the oral mucosal tissue were

increased, indicating that PAD regulated VEGF expression in a concentration-dependent manner. Meanwhile, it was observed that the recovery of ulcer symptoms was accelerated with an increase in PAD dose because VEGF supports angiogenesis and affects wound healing.

To investigate the mode of action of PAD in the treatment of ROU, we investigated the expression of relevant factors in the PAD-mediated TLR4/NF-κB signaling pathway. The NF-κB transcription factor family is a significant regulator that affects both innate and adaptive immunity, as well as inflammatory reactions. It regulates the expression of cytokines, including IL-2, IL-6, IL-10, and TNF-α, as well as the expression of immunoglobulin superfamily adhesion molecules[44,45]. The p50/p65 heterodimer, the most common NF-κB dimer, binds to specific binding sites to control the transcription and expression of downstream-related genes. IκB (IκBα, IκBβ, and IκBε subtypes) inhibits NF-κB activity; this inhibition occurs regardless of the subtype involved and causes NF-κB to remain in a resting state. IKK primarily comprises two catalytic subunits, IKKα and IKKβ, as well as a regulatory subunit, IKKγ. As an IκB kinase, IKK catalyzes IκB phosphorylation, and IκB and IKK participate in inflammatory and immune responses by activating NF-κB. Tissue cells are stimulated by inflammatory cytokines (TNF-α, IL-6, among others) and external pathogens such as bacteria and lipopolysaccharides. These inflammatory cytokines enable TLR4 to transmit extracellular signals via the intracellular MyD88 cascade, thus activating TRAF6 and IκB kinase. They induce phosphorylation and degradation of IκBα and disrupt the resting state of NF-κB and IκBα conjugates. The liberated NF-κB travels from the cytoplasm into the nucleus, where it attaches to the target DNA, initiates the transcription of related genes, and promotes the release of numerous pro-inflammatory cytokines[46]. Therefore, the activity of the TLR4/NF-κB signaling pathway can reflect the inflammatory level of the organism, and inhibiting its activity can alleviate the disease to a certain extent. During tissue injury, activated NF-κB can stimulate VEGF secretion, encourage epithelial cell migration and proliferation, and enhance the formation of vascular tubules[47]. The TLR4/NF-κB signaling pathway is closely linked to the occurrence of ROU. In patients with ROU, changes in TLR4 levels can activate this pathway and release a lot of pro-inflammatory cytokines like TNF-α and IFN-γ, increasing the permeability of oral mucosa and causing local necrosis of oral mucosa[48]. Our findings showed that in the oral mucosa of the model, TLR4, MyD88, TRAF6, NF-κB p50, NF-κB p65, IκBα, and IKKβ expression was significantly upregulated by TLR4/NF-κB pathway mediators, consistent with prior clinical research results[49]. PAD administration significantly downregulated the expression of TLR4/NF-κB pathway mediators, indicating that PAD can inhibit TLR4/NF-κB signaling, relieve the inflammatory state of ROU, and promote tissue neogenesis to exert a therapeutic effect on ROU.

Inflammation is closely associated with oxidative stress. Exposure to harmful external stimuli causes a serious imbalance in the production and elimination of free radicals, destroys the structure and function of biological macromolecules such as nucleic acids, and triggers cell dysfunction and inflammation, thus activating a series of inflammatory responses[50,51]. CAT is an antioxidant enzyme that defends the body against peroxidative states and decomposes H_2O_2 into water and oxygen[52]. GSH and its precursors are intracellular non-protein sulfhydryl antioxidants that can scavenge endogenous ROS and regulate the intracellular oxidative and antioxidant balance, thus protecting cells from oxidation-induced apoptosis, and they act as indicators for evaluating cellular redox status[53]. SOD is primarily present in aerobic metabolic cells, can catalyze O_2 to produce H_2O_2 and O_2. When an organism is under oxidative stress, SOD scavenges free radicals in a timely manner to prevent them from damaging the cells[54,55]. The integrity of the antioxidant defense system is reflected in GSH and SOD, and their serum levels reflect the comprehensive performance of the antioxidant function of the body[56]. L-arginine produces NO, which is catalyzed by non-calcium-dependent NO synthase. This enzyme coordinates and regulates a range of physiological functions in the body, participates in the transduction of several signaling pathways, and binds with superoxide anions to cause oxidative damage to cells[57–59]. Levels of MDA, the final product of lipid peroxidation, can indirectly indicate the severity of oxidative damage[12]. The oxidative stress index of patients with ROU was significantly higher than in the control (healthy volunteers without ROU)[60]. This implies that oxidative stress is essential to the pathogenesis of ROU. Here, compared with the control, serum CAT and oral mucosal mRNA levels were significantly lower in the model ($P < 0.01$). The possible reason was that H_2O_2 produced by the highly active SOD indirectly reduced CAT activity[61]. In addition, the and serum GSH, SOD, NO, and MDA levels were significantly higher ($P < 0.05$), suggesting that the model exhibited oxidative stress damage in the peroxidized state, consistent with clinical findings[62]. After oral administration of PAD, CAT content was significantly elevated relative to the model ($P < 0.05$), while GSH, SOD, NO, and MDA levels were significantly reduced ($P < 0.05$), indicating that PAD could maintain the oxidative balance of the organism and effectively ameliorate oxidative stress injury in ROU rats.

Furthermore, relative to the control group, we observed a significant reduction in the mRNA and protein expression levels of Nrf2, Keap1, NQO1, and HO-1 in the oral mucosal tissue of the model group ($P < 0.01$). This implies that the control of oxidative homeostasis in the oral mucosa of ROU rats is mediated by the Nrf2/HO-1 signaling pathway. Antioxidant enzyme secretion is regulated via the Nrf2 signaling pathway, and these enzymes protect normal cells from oxidative stress and exogenous damage in vivo. They effectively eliminate harmful substances such as ROS and MDA[63]. When subjected to electrophilic stimulation or oxidative stress, Keap1 is inactivated, breaking its connection with Nrf2. Nrf2 is thus activated and moves into the nucleus, where it attaches to antioxidant response elements to trigger the transcription of the antioxidant genes GSH, HO-1, and NQO1. This leads to upregulation of cytokine expression and lessening of oxidative stress damage[64,65]. The antioxidant enzyme HO-1 breaks down heme into Fe^{2+}, CO, and biliverdin, exerting a cytoprotective effect and ameliorating oxidative stress damage[66]. CO from HO-1 stimulates vasodilation to heal ulcers, improves microcirculation at the margins of ulcer lesions, and protects cells from apoptosis. NQO1, an inducible antioxidant flavoprotein that catalyzes the reduction of different reactive species, directly scavenges superoxide and acts alongside HO-1 to preserve the redox state of cells in reaction to inflammatory stimuli and oxidative damage[67].

In the presence of oxidative stress, Nrf2 is activated, leading to the production of SOD and HO-1, two downstream antioxidant enzymes. This accelerates the scavenging of excessive quantities of oxidizing substances such as ROS and MDA, promotes the generation of antioxidant enzymes such as SOD and GSH, improves total antioxidant capacity, and protects the organism from damage[68,69].

PAD significantly upregulated the mRNA and protein expression of Nrf2, Keap1, NQO1, and HO-1 ($P < 0.05$). This indicates that PAD induces Nrf2 to synthesize and secrete downstream detoxification enzymes (HO-1 and NQO1) by activating the Nrf2/HO-1 signaling pathway. This regulates the antioxidant capacity of the body and alleviates oral antigen emulsifier-induced oxidative damage of the oral mucosal tissues in ROU rats.

In summary, PAD can regulate the proportions of $CD3^+$ and $CD4^+$ cells and the $CD4^+/CD8^+$ ratio in peripheral blood and serum IgA, IgG, and IgM levels, restoring them to normal levels and maintaining the balance of immune function. PAD alleviates the inflammatory state of the oral mucosa in ROU rats by promoting IL-2 and IL-10 expression and inhibiting IL-6, TNF-α, and IL-1β expression. Additionally, PAD promotes VEGF expression and the growth of granulation tissue to accelerate the repair of oral ulcer wounds. Moreover, PAD can balance immunity and oxidative stress in ROU rats by activating Nrf2/HO-1 signaling and deactivating TLR4/NF-κB signaling. The effects of PAD, therefore, have implications for the treatment of ROU.

Materials and methods

Drugs and reagents

Levamisole hydrochloride (LM) tablets were purchased from Shandong Renhetang Pharmaceutical Co., Ltd. (Shandong, China). The following products were purchased: Complete Freund's adjuvant (SLCH1443; Sigma-Aldrich, St. Louis, MO, USA); phosphate-buffered saline (PBS; GP21030202721; Servicebio, Wuhan, China); PerCP/Cyanine5.5 anti-rat CD3 and APC anti-rat CD8a (B329872 and B316147, respectively; BioLegend, San Diego, CA, USA); Anti-rat CD4, eBioscience FITC and TRIzol Reagent (2,174,911 and 15,596,026, respectively; Invitrogen, Carlsbad, CA, USA). Assay kits for IgA, IgG, IgM, IL-2, IL-6, IL-10, vascular endothelial growth factor (VEGF), TNF-α, catalase from Micrococcus lysodeikticus (CAT), glutathione (GSH), superoxide dismutase (SOD), nitric oxide (NO), and malondialdehyde (MDA) were purchased from Nanjing Jiancheng Bioengineering Institute, China. The other reagents and kits used were the RevertAid First Strand cDNA Synthesis Kit (00,906,776; Thermo Fisher Scientific, Waltham, MA, USA), TB Green Premix Ex Taq II (AL31516A; TaKaRa, Tokyo, Japan), RIPA lysis buffer, SDS-PAGE sample loading buffer (5×), BeyoColor™ prestained color protein marker (Beyotime Biotechnology, China), Red blood cell lysis buffer, Heparin sodium, DEPC-water (DNase, RNase free), Protein phosphatase inhibitor (All-in-one, 100×), BCA protein assay kit, SDS-PAGE gel kit, Tris (hydroxymethyl) aminomethane, glycine (Solarbio, China), polyvinylidene difluoride (PVDF) Western blotting membranes (R1CB66018; Millipore, Billerica, MA, USA), Sodium dodecyl sulfate (SDS; Shanghai Regal Biology Technology Co, Ltd, China), and Bovine serum albumin (BSA; EZ4567D106; BioFroxx, Frankfurt, Germany). The following antibodies were used: Rabbit monoclonal antibodies against GAPDH, NF-kappaB p65 (NF-κB p65), MyD88, Keap1, and HO-1 (5174S, 8242S, 4283S, 8047S, 82206S; Cell Signaling Technology, Danvers, MA, USA); rabbit monoclonal antibodies against NF-κB p50, IκBα, TRAF6, and NQO1; and rabbit polyclonal-antibodies against TLR4 and Nrf2 (ab32360, ab32518, ab33915, ab80588, ab217274, and ab92946, respectively; Abcam, Cambridge, UK); HRP-conjugated AffiniPure Goat Anti-Rabbit IgG (H + L; HRP-IgG; sa00001-2; Proteintech, Wuhan, China).

Details on *P. americana* and PAD preparation

The medicinal material of *P. americana* was purchased from Yunnan Jingxin Biotechnology Co., Ltd. (20,210,311, Yunnan, China) and was identified as *P. americana* L. by Dr. Zizhong Yang (Yunnan Provincial Key Laboratory of Entomological Biopharmaceutical R&D, Dali University).

PAD was prepared using the extraction and purification process described in previous studies by our research group (Patent No. CN201410524173.3). *P. americana* was dried and crushed, and the coarse powder was extracted three times with 60% ethanol at 70–80 °C for three hours each cycle after being sieved through a 24-mesh sieve. The extract was then filtered, collected, concentrated under reduced pressure, and defatted. The degreased solution was used in activated carbon column chromatography and eluted with 80% ethanol. Finally, the eluent was collected and concentrated into an extract with a density of approximately 1.30 g/mL, producing the final PAD. This PAD is used in "Yunnan Baiyao toothpaste" (QB/T5287-218).

Examination of the chemical composition in PAD by UPLC-Q-TOF–MS

PAD was ultrasonically mixed at low temperature in methanol: acetonitrile: water (2: 2: 1, v/v). Subsequently, it was centrifuged at 14,000 × *g* at 4 °C for 20 min. Following centrifugation, the supernatant was collected and vacuum-freeze dried. The samples were then redissolved in a 1:1 v/v acetonitrile to water solution, then centrifuged at 14,000 × g for 15 min at 4 ℃. The supernatant was removed and injected into a UPLC-Q-TOF–MS (Agilent UHPLC, USA) analyzer (Shenzhen Weike Meng Technology Group Co. Ltd., Shenzhen, China).

Constructing the ROU rat model and drug administration

Seventy-eight male SD rats (Specific Pathogen Free; weight 190–210 g) were purchased from Hunan SJA Laboratory Animal Co., Ltd. (Hunan, China; license number: SCXK [Xiang]-2019–0004; experimental animal quality Certificate No. 430727210101391728). The experimental protocol was approved by the Laboratory Animal Ethics Committee of Dali University (Approval no. 2019-PZ-078). The rats were housed in separate cages under SPF conditions at 22–25 °C and 50–60% humidity. During the experiment, the cages were cleaned, bedding materials were regularly changed, and the rats were given basic feed and cold boiled water while observing the principles of experimental animal use and management.

The experiment was carried out after 1 week of adaptive feeding. Forty-eight rats were randomly separated into 6 groups according to body weight: control group, model group, positive drug group (LM group), and PAD low-, medium-, and high-dose groups (PAD-L, PAD-M, and PAD-H), with 8 rats in each group. The remaining 30 rats were used to prepare an oral mucosal tissue homogenate (mixed with the same homogenate volume with complete Freund's adjuvant to prepare the antigen emulsifier).

Spinal hair removal was performed on both sides of rats in each group, followed by routine disinfection. The control group rats were subcutaneously injected with complete Freund's adjuvant on both sides of the spine where the hair was removed. In contrast, the other groups were injected with the antigen emulsifier at the same site to establish a rat model of ROU. The injection dose was 0.1 mL per side once a week for 6 weeks. After successful modeling, the animals in the LM group were given LM tablets orally (20 mg/kg); the PAD-L, PAD-M, and PAD-H groups were treated with PAD (0.2812, 0.5625, and 1.125 g/kg, respectively); and the control and model groups were administered an equal volume of 0.9% normal saline once a day for 7 days.

Observation of ulcer symptoms in rats

Following a 7-day medication regimen, Symptoms of oral ulcers were observed and recorded visually, including the number and duration of ulcers, and the size of oral ulcers in each group was measured by vernier calipers.

Collection and preparation of experimental samples

Following a 7-day medication regimen, the animals were fasted for 24 h with free access to water. Subsequently, the animals were euthanized by anesthesia with 1% sodium pentobarbital according to body weight, and blood samples were collected. The collected blood samples were allowed to stand and centrifuged at 2000 × *g* for 10 min to separate the upper serum. The serum was sub-packaged, labeled, and stored at − 80 °C for subsequent Enzyme-linked immunosorbent assay (ELISA) and detection of oxidative stress indices. After blood collection, the oral mucosa of the rats was peeled off, and other tissues surrounding the mucosa were removed. Part of the mucosa was immersed in 4% paraformaldehyde for fixation, while the remaining portion was preserved at − 80 °C for subsequent use. All the animal procedures used in this study were in accordance with the protocols of the National Institute of Health Guide for the Care and Use of Laboratory Animals and ARRIVE guidelines. The permission (Approval no. 2019-PZ-078) was obtained from the Laboratory Animal Ethics Committee of Dali University and conducted in accordance with the guidelines set by the National Institutes of Health and the Animal Care and Use Ethics Committee of Dali University, China.

Histopathological observation of oral mucosa

The oral mucosal tissue was fixed in 4% paraformaldehyde, embedded in paraffin, and sliced into 5-μm-thick sections. After dewaxing treatment and hematoxylin–eosin (HE) staining, the slices were dehydrated and sealed. Pathological changes in the oral mucosa were observed, and the images were recorded under an optical microscope (OLYMPUS, Japan).

Detection of immune indexes in peripheral blood using flow cytometry

Blood samples were taken from the orbital venous plexus of the anesthetized rats. Erythrocyte lysate was added to 100 μL of the anticoagulated whole blood, which was then lysed and centrifuged at low speed to obtain cell precipitates. PBS containing Fetal Bovine Serum was added to the precipitate to wash and resuspend the cells; this was performed twice. Then, PerCP/Cyanine5.5 anti-rat CD3, anti-rat CD4, eBioscience FITC, and APC anti-rat CD8a antibodies were added, and the cell samples were incubated in an ice box for 30 min away from light. After incubation, the cells were passed through a 200-mesh sieve and twice washed with PBS; levels of $CD3^+$, $CD4^+$, $CD8^+$, and $CD4^+/CD8^+$ were determined by flow cytometry (Becton, Dickinson, and Company, USA), and the data were recorded. The data were analyzed using FlowJo Version 10 analysis software.

Detection of immunoglobulins and cytokines in serum using ELISA

Serum levels of the immune indicators IgA, IgG, and IgM and of the cytokines VEGF, IL-2, IL-6, IL-10, and TNF-α were detected per the ELISA kit instructions.

Detection of serum oxidative stress index

After thawing the serum, the optical density values of CAT, GSH, SOD, NO, and MDA were measured at the required wavelengths using a Multifunctional enzyme labeling instrument (Bio Tek Instruments, Inc., USA) according to the operating procedures of the kit.

Immunohistochemical staining of oral mucosa tissue

The oral mucosa slices were dewaxed and hydrated, then washed with PBS and treated with 3% H_2O_2 at 37 °C for 30 min to inhibit endogenous peroxidase activity. After that, the slices were incubated in 5% BSA solution for 30 min, followed by incubation at 4 °C overnight with the corresponding primary antibodies (anti-IκBα, anti-NF-κB p50, anti-Keap1, anti-NQO1, and anti-HO-1). Following the primary antibody incubation, the sections underwent a PBS wash and were subsequently incubated for 60 min with a secondary antibody (HRP peroxidase-conjugated IgG). After incubation, the slices were visualized using diaminobenzidine, counterstained with HE, dehydrated, and sealed with neutral glue. The IκBα, NF-κB p50, Keap1, NQO1, and HO-1 stainings were evaluated under an optical microscope (OLYMPUS, Japan). Using Image-Pro Plus 6.0 image analysis software, the IHC results of the oral mucosa were analyzed. The relative protein expression level was determined by averaging the optical density value of the positive results.

Primer name		Primer sequence (5′ to 3′)
GAPDH	F	GGGGCTCTCTGCTCCTCCCTG
	R	CGGCCAAATCCGTTCACACCG
IL-1β	F	TCTGACAGGCAACCACTTAC
	R	CATCCCATACACACGGACAA
TNF-α	F	AAAGGACACCATGAGCACGGAAAG
	R	CGCCACGAGCAGGAATGAGAAG
VEGF	F	CTGCTGTGGACTTGAGTTGG
	R	CAAACAGACTCCGGCCTCTC
TLR4	F	TCCACAAGAGCCGGAAAGTT
	R	TGAAGATGATGCCAGAGCGG
IKKβ	F	AGGAAGACTGTAACCGGCTG
	R	CCGTTCTACCAGGACCTTCAC
NF-κB p50	F	GATGGGACGACACCTCTACACATA
	R	CCCAAGAGTCGTCCAGGTCA
NF-κB p65	F	CTGCCGGGATGGCTTCTATG
	R	TATTGTTGGTCTGGATGCGCT
IκBα	F	AGACTCGTTCCTGCACTTGG
	R	TCTCGGAGCTCAGGATCACA
Nrf2	F	GCACATCCAGACAGACACCA
	R	CTCTCAACGTGGCTGGGAAT
Keap1	F	ACCGCTACGTGGAGACAGA
	R	GTCATAGCATTCCACACTGTCCAG
NQO1	F	CCACGCAGAGAGGACATCAT
	R	TCAGATTCGACCACCTCCCA
HO-1	F	CCACGCATATACCCGCTACC
	R	CGATGCTCGGGAAGGTGAAA
CAT	F	ACTGACGTCCACCCTGACTA
	R	CCCTTGGCAGCTATGTGAGA

Table 2. Primer sequences for qRT-PCR.

Quantitative RT-PCR detection of target gene expression

An ultramicro nucleic acid protein analyzer (Thermo Fisher Scientific) was used to measure the purity and concentration of total mRNA that was isolated from the oral mucosa using the TRIzol technique. Using a RevertAid first-strand cDNA synthesis kit, RNA was reverse-transcribed into complementary DNA (cDNA) following the manufacturer's instructions. The CFX96 Real-Time PCR Detection System (qRT-PCR; Bio-Rad Laboratories, Hercules, CA, USA) was used to determine the mRNA levels. The PCR reaction process consisted of 49 cycles: predenaturation at 95 °C for 30 s, reaction at 95 °C for 5 s, and reaction at 60 °C for 30 s. Using GAPDH as the internal reference, we utilized the $2^{-\Delta\Delta Ct}$ method to quantify the relative expression of the target gene. The corresponding primer sequences (synthesized by Sangon Biotech Co., Ltd., Shanghai) are listed in Table 2.

Western blot detection of protein expression in oral mucosal tissue

Approximately 100 mg of the rat oral mucosa samples were added to RIPA lysis buffer, ground, and lysed, and the supernatant was then separated by centrifugation. The BCA protein assay kit was used to measure the amount of protein in the supernatant. Proteins were deposited onto a PVDF membrane after being separated by sodium dodecyl sulfate–polyacrylamide gel electrophoresis. The PVDF membrane was sealed with 5% BSA at 20 ± 3 °C for 2 h, and then incubated in the primary antibody (GAPDH, 1:1000; TLR4, 1:1000; MyD88, 1:1000; TRAF6, 1:2000; NF-κB p50, 1:1000; NF-κB p65, 1:1000; IκBα, 1:5000; Nrf2, 1:1000; Keap1, 1:1000; NQO1, 1:10,000; HO-1, 1:1000) on a shaking table at 4 °C for 13 h. Subsequently, the PVDF membrane was cleaned five times with Tris Buffered Saline Tween (TBST) for 5 min washes each time, placed in a second antibody (HRP-IgG, 1:5000), and incubated on a shaker at 20 ± 2 °C for 1 h. Following an additional TBST wash, the membrane was developed using an appropriate amount of developer. Western blotting results were analyzed using ImageJ software. The ratio of the target protein's average optical density value to that of the internal reference protein (GAPDH) was used to determine the relative expression levels of the proteins.

Statistical analysis

Data processing and statistical analysis were done with SPSS 22.0 (SPSS Inc., Chicago, IL, USA). The findings are presented as mean ± standard deviation and inter-group comparisons were conducted using one-way ANOVA. Differences were considered statistically significant at $P < 0.05$.

Data availability

Data is provided within the manuscript or supplementary information fles.

Glossary

PAD	*Periplaneta americana* extract
ROU	Recurrent oral ulcer
BCA	Bicinchoninic acid assay
BSA	Bovine serum albumin
CAT	Catalase from *Micrococcus lysodeikticus*
DEPC	Diethyl pyrocarbonate
ELISA	Enzyme-linked immunosorbent assay
GSH	Glutathione
HE	Hematoxylin-eosin staining
HO-1	Hemoxygenase-1
IL-10	Interleukin-10
IL-1β	Interleukin-1β
IL-2	Interleukin-2
IL-6	Interleukin-6
IκBα	Inhibitor of nuclear factor-kappa B alpha
Keap1	Kelch-like ECH-associated protein 1
MDA	Malondialdehyde
MyD88	Myeloid differentiation factor 88
NF-κB p50	Nuclear factor-kappa B p50
NF-κB p65	Nuclear factor-kappa B p65
NO	Nitric oxide
NQO1	NADPH: quinone oxidoreductase
Nrf2	Nuclear factor erythroid 2-related factor 2
PVDF	Polyvinylidene difluoride
SOD	Superoxide dismutase
TLR4	Toll-like receptor 4
TNF-α	Tumor necrosis factor-alpha
TRAF6	TNF receptor-associated factor 6
VEGF	Vascular endothelial growth factor

Received: 24 August 2024; Accepted: 26 December 2024
Published online: 12 March 2025

References

1. Ruan, H. H. et al. Frequencies of abnormal humoral and cellular immune component levels in peripheral blood of patients with recurrent aphthous ulceration. *J. Dent. Sci.* **13**(2), 124–130. https://doi.org/10.1016/j.jds.2017.09.003 (2018).
2. Slebioda, Z., Szponar, E. & Kowalska, A. Etiopathogenesis of recurrent aphthous stomatitis and the role of immunologic aspects: literature review. *Arch. Immunol. Ther. Exp. (Warsz).* **62**(3), 205–215. https://doi.org/10.3892/br.2019.1221 (2014).
3. Rivera, C. Essentials of recurrent aphthous stomatitis. *Biomed. Rep.* **11**(2), 47–50. https://doi.org/10.3892/br.2019.1221 (2019).
4. Elias, M. L., Fatahzadeh, M. & Schwartz, R. A. Recurrent aphthous stomatitis: An enigmatic entity and sign of systemic disease. *Indian J. Dermatol.* **67**(6), 834. https://doi.org/10.4103/ijd.ijd_971_20 (2022).
5. Mimura, M. A. M., Borra, R. C., Hirata, C. H. W. & de Oliveira Penido, N. Immune response of patients with recurrent aphthous stomatitis challenged with a symbiotic. *J. Oral Pahol. Med.* **46**(9), 821–828. https://doi.org/10.1111/jop.12621 (2017).
6. Chiang, C. P. et al. Recurrent aphthous stomatitis - Etiology, serum autoantibodies, anemia, hematinic deficiencies, and management. *J. Formos. Med. Assoc.* **118**(9), 1279–1289. https://doi.org/10.1016/j.jfma.2018.10.023 (2019).
7. Lee, Y. C., Jeong, S. J., Eun, Y. G., Song, R. & Oh, I. H. Risk of autoimmune diseases in recurrent aphthous ulcer patients: A nationwide population study. *Oral Dis.* **27**(6), 1443–1450. https://doi.org/10.1111/odi.13659 (2021).
8. Shen, C. L. et al. Serum interleukin-6, interleukin-17A, and tumor necrosis factor-alpha in patients with recurrent aphthous stomatitis. *J. Oral Pathol. Med.* **50**(4), 418–423. https://doi.org/10.1111/jop.13158 (2021).
9. Zhen, X. H., Dong, B., Yuan, P. W. & Zhen, J. Research progress of NF-κB signaling pathway in cartilage destruction in osteoarthritis. *J. Chin. J. Pain Med.* **27**(07), 540–544 (2021).
10. Afonina, I. S., Zhong, Z., Karin, M. & Beyaert, R. Limiting inflammation-the negative regulation of NF-κB and the NLRP3 inflammasome. *J. Nat. Immunol.* **18**(8), 861–869. https://doi.org/10.1038/ni.3772 (2017).
11. Gao, S. et al. Histidine-rich glycoprotein ameliorates endothelial barrier dysfunction through regulation of NF-κB and MAPK signal pathway. *J. Br. J. Pharmacol.* **176**(15), 2808–2824. https://doi.org/10.1111/bph.14711 (2019).
12. Guan, C. Q., Guo, H. B., Wu, Y. X. & Yuan, Z. Y. Oxidative stress and cellular immune status in patients with recurrent oral ulcer. *J. Chin. Rem. Clin.* **18**(06), 884–885 (2018).
13. Mei, S. Y., Zhang, Y. M., Gao, Q. F. & Zhang, Y. T. Effects of soybean agglutinin on oxidative stress and inflammatory factors in rabbit small intestines. *J. Chin. Feed.* **01**, 66–70. https://doi.org/10.15906/j.cnki.cn11-2975/s.2023020011-01 (2024).
14. Lu, X. Y. et al. Pomegranate peel extract ameliorates colitis by reducing inflammation and oxidative stress in mice. *J. Shanxi Med. Univ.* **55**(01), 50–56. https://doi.org/10.13753/j.issn.1007-6611.2024.01.007 (2024).
15. Zhang, X. Z., Du, Y., Fan, Y. S. & Bao, J. To explore the pathogenesis and TCM prevention and treatment of "aphthous ulcer" based on the theory of oxidative stress. *J.Zhejiang J. Integr. Tradit. Chin. West. Med.* **28**(02), 150–152 (2018).
16. Huang, H.F., Pang, X.Y., Dai, W.B., Huang, M.T. & Zeng, C.Y. Study on the Protective Effect and Mechanism of Chai Hu Shu Gan Granules onTetrachloromethane-Induced Acute Liver Injury Model Mice. J. Chin. Pharma. J. 1–16. http://gfffgbd0802d1f56e4a16scu5ox0xfuqvu6f5x.fffg.dali.cwkeji.cn/urlid/11.2162.R.20240228.1740.002 (2024).
17. Chen, Y. et al. Periplaneta Americana extract plays an anti-fibrosis role in inhibiting oxidative stress via Nrf2/HO-1 pathway. *J.Chin. J. Hosp. Pharm.* **42**(04), 367–372. https://doi.org/10.13286/j.1001-5213.2022.04.05 (2022).
18. Gao, Y. et al. Chemical constituents from Periplaneta Americana. *J. Chin. Tradit. Pat. Med.* **40**(02), 375–378 (2018).

19. Gao, J. et al. Research progress on the tissue repair mechanism of Periplaneta Americana extract. *J. Sichuan J. Zool.* **38**(02), 235–240 (2019).
20. Wang, Q., Liu, K. N., Kong, C. H., Zhang, C. G. & Sui, S. Y. Research progress on extraction and Pharmacological activities of effective constituents from Periplaneta Americana. *J. Chin. Arch. Tradit. Chin.* **39**(08), 108–111. https://doi.org/10.13193/j.issn.1673-7717.2021.08.024 (2021).
21. Wang, P. W., Yang, F. & Cao, W. Q. Research progress on clinical application of Chinese medicine Periplaneta Americana LinnaeusExtract Kangfuxin solution at home and abroad. *J. Pharm. Today.* **33**(10), 784–788 (2023).
22. Wang, L. The effect of kangfuxin liquid in the treatment of radiation oral ulcers and its effect on Patientslmmune function and inflammatory factor levels. *J. Guide China Med.* **19**(28), 120–121. https://doi.org/10.15912/j.cnki.gocm.2021.28.049 (2021).
23. Tan, Q. Y., Man, H. X., Na, K. G., Yang, Y. S. & Xiao, P. Y. Effect of the Periplaneta Americana extract on oral ulcer in rats. *J. Chin. J. Clin. Pharmacol.* **32**(11), 1014–1016. https://doi.org/10.13699/j.cnki.1001-6821.2016.11.017 (2016).
24. Xu, Z. L., Wang, L., Jin, Y. X. & Hou, J. Z. Research progress in recurrent oral ulcer and level changes of related lmmune factors. *J. Med. Recapitul.* **27**(24), 4893–4897 (2021).
25. Xu, J. B., Wang, D. D., Peng, X. L., Song, F. X. & Wang, C. D. Changes and significance of oral flora,serum inflammatory factors,and T cell subgroup levels inpatients with recurrent oral ulcers. *J. Mol. Diagn. Ther.* https://doi.org/10.19930/j.cnki.jmdt.2021.09.029 (2021).
26. Zou, Y. H., Yang, J. & Chen, C. H. Correlation of TNF-a, lL-2,6 and immune function with recurrent oral ulcers. *J. Hainan Med. Univ.* **21**(09), 1299–1301. https://doi.org/10.13210/j.cnki.jhmu.20150505.005 (2015).
27. Ma, X. Z. et al. Expression and significance of lL-12 and lL-12R in patients with recurrent oral ulcer. *J. Chin. J. Clin.(Electro. Edit.)* **8**(16), 2931–2934 (2014).
28. Ke, Q. K. Curative effect of levamisole hydrochloride in the treatment of refractory pneumonia in children. *J. Shenzhen J. Integr. Tradit. Chin. West. Med.* **27**(22), 104–106. https://doi.org/10.16458/j.cnki.1007-0893.2017.22.054 (2017).
29. Qi, J., Yu, Z. H., Liu, Y. & Bo, L. Establishment of Rats' Recurrent Aphthous Ulcer with Immunology. *J. Oral Sci. Res.* **26**(06), 816–819. https://doi.org/10.13701/j.cnki.kqyxyj.2010.06.021 (2010).
30. Mi, X. Relationship between the clinical features of recurrent aphthous ulcerand serum levels of cellular immunity and humoral immunity. *D. Ningxia Med. Univ.* https://doi.org/10.27258/d.cnki.gnxyc.2021.000136 (2021).
31. Lan, Y. L., Tang, L. & Cui, R. L. Study on the changes of iron metabolism in patients with recurrent oral ulcer and its relationship with cellular immune function. *J. Shanghai J. Stomatol.* **26**(3), 302–304. https://doi.org/10.19439/j.sjos.2017.03.015 (2017).
32. Shang, Z. Z., Wang, A. A., Gao, X. T. & Liu, T. H. Progress in the etiology of recurrent oral ulcers. *J. Electron. J. Gen. Stomatol.* **6**(19), 26–27. https://doi.org/10.16269/j.cnki.cn11-9337/r.2019.19.017 (2019).
33. Chen, Y. D., Yang, H., Qiu, H. S. & Ma, L. D. Changes of serum TNF-α, IL-2 and T lymphocytes in patients with recurrent oral ulcer. *J. Hainan Med. J.* **28**(01), 94–95 (2017).
34. Li, H. & Li, H.Q. Changes in immune indexes, iron metabolism and TNF-alpha levels in patients with recurrent oral ulcers. J. China J. Mod. Med. **30**(01) 41–44https://link.cnki.net/urlid/43.1225.r.20200110.0843.016 (2020).
35. Wang, L. P. & Pan, Y. J. Correlation between lL-2 and lL-6 in ear effusion and $CD4^+/CD8^+$ in peripheral blood of patients secretory otitis media. *J.J. Hunan Norm. Univ. (Med. Sci.)* **16**(05), 184–187 (2019).
36. Fatkhullina, A. R., Peshkova, I. O. & Koltsova, E. K. The role of cytokines in the development of atherosclerosis. *J. Biochem. (Mosc)* **81**(11), 1358. https://doi.org/10.1134/S0006297916110134 (2016).
37. Sun, W. L. et al. Polymorphism of Pro-lnflammatory Factors(lL-1B, lL-6, TNF-α) in Tibetan Pigs and Its Association with lmmune Traits Analysis. J. Acta Veterinaria et Zootechnica Sinica. 1–13. (2024).
38. Bender, O., Weinberg, E., Moses, O., Nemcovsky, C. E. & Weinreb, M. Porphyromonas gingivalis lipopolysaccharide and glycated serum albumin increase the production of several pro-inflammatory molecules in human gingival fibroblasts via NFκB. *Arch. Oral Biol.* **116**, 104766. https://doi.org/10.1016/j.archoralbio.2020.104766 (2020).
39. Mousa, A. M. et al. Antiulcerogenic effect of Cuphea ignea extract against ethanol-induced gastric ulcer in rats. *BMC Complement. Altern. Med.* **19**(1), 345 (2019).
40. Chaudhuri, K., Nair, K. K. & Ashok, L. Salivary levels of TNF-α in patients with recurrent aphthous stomatitis: A cross-sectional study. *J. Dent. Res. Dent. Clin. Dent. Prospect.* **12**(1), 45–48 (2018).
41. Mei, H. P. et al. Effect of dilian erxin granule on MCP-1/CCR2/NF-κB signaling pathway and expression of inflammatory factors after recurrent oral ulcer in rats. *J. Bachu Med. J.* **1**(01), 16–22 (2018) (**+34**).
42. Li, J. X. et al. Effects of conditioned medium of ADSCs transfected with VEGF on dermal fibroblasts andumbilical vein endothelial cells in vitro. *J. Chin. J. Pathophysiol.* **35**(03), 542–548 (2019).
43. Sui, L. et al. Study on application of one-stage double-layer artificial dermis combined with VSD in treatment of large-area bone/tendon exposure wounds of lower limbs. *J. Chin. J. Coal Ind. Med.* **27**(01), 73–77 (2024).
44. Mafra, C. A. D. C. C. et al. Gliclazide prevents 5-FU-Induced oral mucositis by reducing oxidative stress, inflammation, and p-selectin adhesion molecules. *Front. Physiol.* **10**, 327. https://doi.org/10.3389/fphys.2019.00327 (2019).
45. Jayaganesh, R., Pugalendhi, P. & Murali, R. Effect of citronellol on NF-κB inflammatory signaling molecules in chemical carcinogen-induced mammary cancer in the rat model. *J. Biochem. Mol. Toxicol.* **34**(3), e22441 (2020).
46. Qi, Q. et al. Effect of Tongluo Juanbi Granule on Inflammatory Injury and Apoptosis of Osteoarthritis Based onTLR4/MyD88/NF-κB Pathway. *J. Chin. J. Exp. Tradit. Med. Form.* **24**, 1–9 (2024).
47. Butler, C. T. et al. A Quininib Analogue and Cysteinyl Leukotriene Receptor Antagonist Inhibits Vascular Endothelial Growth Factor (VEGF)-independent Angiogenesis and Exerts an Additive Antiangiogenic Response with Bevacizumab. *J. Biol. Chem.* **292**(9), 3552–3567. https://doi.org/10.1074/jbc.M116.747766 (2017).
48. Chen, K. Q., Tan, W. C., Yu, L. X., Wan, S. & He, X. F. Effects of duyiwei capsule on lmmune function and protein expression of NF-kB inflammatorypathway in ulcer tissue of rats with recurrent oral ulcer. *J. Prog. Mod. Biomed.* **22**(16), 3020–3024 (2022).
49. Zhang, J. et al. Relationship between nuclear factor-κB signaling pathway and susceptibility of recurrent aphthous ulcer. *J. Shanghai J. Stomatol.* **27**(05), 513–517 (2018).
50. Bagan, J. et al. Oxidative stress and recurrent aphthous stomatitis. *Clin. Oral Investig.* **18**(8), 1919–1923. https://doi.org/10.1007/s00784-013-1181-2 (2014).
51. Zhang, Z. C., Li, S. & Fang, H. Q. Enzymatic antioxidants status in patients with recurrent aphthous stomatitis. *J. Oral Pathol. Med.* **46**(9), 817–820 (2017).
52. Babaee, N. et al. Salivary oxidant/ antioxidant status and hematological parameters in patients with recurrent aphthous stomatitis. *Casp. J. Intern. Med.* **7**(1), 13–18 (2016).
53. Sami, G. et al. Effect of corticosteroid (triamcinolone acetonide) and chlorhexidin on chemotherapy- induced oxidative stress in buccal mucosa of rats. *Ear Nose Throat J.* https://doi.org/10.1177/0145561319894405 (2020).
54. AlTamimi, J. Z. et al. The protective effect of 11-Keto-β-Boswellic acid against diabetic cardiomyopathy in rats entails activation of AMPK. *Nutrients* **15**(7), 1660. https://doi.org/10.3390/nu15071660 (2023).
55. Doran, M. L. et al. Metabolomic analysis of oxidative stress: Superoxide dismutase mutation and paraquat induced stress in Drosophila melanogaster. *Free Radic. Biol. Med.* **113**, 323–334 (2017).
56. de Araújo, A. A. et al. Azilsartan reduced TNF-α and IL-1β levels, increased IL-10 levels and upregulated VEGF, FGF, KGF, and TGF-α in an oral mucositis model. *PLoS One* **10**(2), e0116799 (2015).
57. Hu, L. F. et al. Anti-oxidative stress actions and regulation mechanisms of Keap1-Nrf2/ARE signal pathway. *J. Int. Pharma. Res.* **43**(01), 146–152 (2016) (**+166**).

58. Picón-Pagès, P., Garcia-Buendia, J. & Muñoz, F. J. Functions and dysfunctions of nitric oxide in brain. *Biochim. et Biophys. Acta (BBA) – Mol. Basis Dis.* **1865**(8), 1949–1967 (2019).
59. Zhu, H. Y., Hong, F. F. & Yang, S. L. The roles of nitric oxide synthase/nitric oxide pathway in the pathology of vascular dementia and related therapeutic approaches. *J. Int. J. Mol. Sci.* **22**(9), 4540 (2021).
60. Ekinci, A., Demir, E. & Ekinci, H. Serum prolidase and oxidative stress levels in patients with recurrent aphthous stomatitis: A prospective, controlled study. *J. Ind. J. Dermatol. Venereol. Leprol.* **86**(1), 18–23 (2020).
61. Xia, B. et al. Effects of chlorantraniliprole and Its metabolite IN-EQW78 on antioxidant and reproductive capacity of earthworms. *J. Asian J. Ecotoxicol.* https://doi.org/10.7524/AJE.1673-5897.20240327002 (2024).
62. Zhang, Z.C. Study on the correlation between oxidative stress and recurrent oral ulcer. Heibei: Bethune international Peace Hospital of PLA. 2016-12-01. (2016).
63. Qiu, M. et al. Protective effect of hedansanqi Tiaozhi Tang against non-alcoholic fatty liver disease in vitro and in vivo through activating Nrf2/HO-1 antioxidant signaling pathway. *J. Phytomed.* **67**, 153140 (2020).
64. Lu, Z.H., Shen, J., Huang, W.J., Sun, W. & Ma, Y.X. SIRT6 overexpression inhibits Ang ll-induced cardiomyocyte apoptosis by regulatingAMPK/Nrf2/HO-1 signaling pathway. J. Chin. J. Arterioscle. 1–9 (2024).
65. Gao, L. N., Zhang, X. & He, J. F. Effect of Genistein on hypoxia/reoxygenation injury of hippocampal neurons by regulatingNrf2/HO-1 signaling pathway. *J. Strok. Nerv. Dis.* **31**(01), 14–20 (2024).
66. Ma, C.J. et al. Effects of Modified Dahuang Huanglian Xiexintang on Oxidative Stress lnjury of Liver in Type 2Diabetes Rats Based on Nrf2/HO-1 Axis. J. Chin. J. Exp. Tradit. Med. Formul. 1–11 (2024).
67. Ross, D. & Siegel, D. Functions of NQO1 in cellular protection and CoQ_{10} metabolism and its potential role as a redox sensitive molecular switch. *J. Front. Physiol.* **8**, 595. https://doi.org/10.1016/j.bbamcr.2014.05.003 (2017).
68. Namani, A., LI, Y., Wang, X. J. & Tang, X. W. Modulation of NRF2 signaling pathway by nuclear receptors: implications for cancer. *Biochim. Biophys. Acta.* **1843**(9), 1875–1885. https://doi.org/10.1016/j.bbamcr.2014.05.003 (2014).
69. Qiu, M. Y. et al. Protective effect of Hedansanqi Tiaozhi Tang against non-alcoholic fatty liver disease in vitro and in vivo through activating Nrf2/HO-1 antioxidant signaling pathway. *Phytomedicine.* **67**, 153140. https://doi.org/10.1016/j.phymed.2019.153140 (2020).

Author contributions

WJL and YC: designed and performed the experiments, analyzed the data, and wrote the original draft of the manuscript. KLL, ZZC, JYZ, GHZ, FFS: analyzed the data. PYX, YSY: designed the experiments, received the funds, and provided guidance for the experiments and manuscript writing. All authors read and approved the fnal manuscript.

Funding

This study was supported by the Yunnan Expert Workstation (grant number 202405AF140044); Joint Project of Basic Research of Local Universities in Yunnan Province (grant number 202401BA070001-007); and Basic Research Key Projects of Science and Technology Department of Yunnan Provincial (grant number 202501AS070162).

Declarations

Competing interests

The authors declare no competing interests.

Ethics approval and consent to participate

This study was approved by the Laboratory Animal Ethics Committee of Dali University (Approval no. 2019-PZ-078).

Additional information

Supplementary Information The online version contains supplementary material available at https://doi.org/10.1038/s41598-024-84703-7.

Correspondence and requests for materials should be addressed to P.X. or Y.Y.